optica

Distributed cladding mode fiber-optic sensor: supplementary material

G. BASHAN, YOSEF LONDON, H. HAGAI DIAMANDI, AVI ZADOK*

*Faculty of Engineering and Institute for Nano-Technology and Advanced Materials, Bar-Ilan University, Ramat-Gan 5290002, Israel *Corresponding author: Avinoam.Zadok@biu.ac.il*

Published 17 January 2020

This document provides supplementary information to "Distributed cladding mode fiber-optic sensor," https://doi.org/10.1364/OPTICA.377610. Mathematical analysis of random-access, dynamic and localized coupling of light the cladding modes of a standard optical fiber is provided. Coupling is based on the stimulation of Brillouin dynamic gratings by two pump tones that counter-propagate in the core mode of the fiber. A third optical probe wave may be reflected by the dynamic grating into a counter-propagating cladding mode. Phase matching and spatial overlap considerations are discussed, and expressions for the magnitude and spectrum of coupling are obtained. The localization of dynamic gratings through phase coding of the pump waves is briefly reviewed.

1. Coupling to cladding modes of a standard single-mode fiber using Brillouin dynamic gratings

Let $E_{\text{pump1}}(r,z,t)$ denote the optical field of a first continuous pump wave, propagating in the single core mode of a standard fiber in the positive $\hat{\mathbf{z}}$ direction:

$$E_{\text{pump1}}(r,z,t) = A_{\text{pump1}}(z)\exp\left(\mathrm{j}k_{\text{pump1}}z - \mathrm{j}\omega_{\text{pump1}}t\right)u_{\text{core}}(r) + c.c \tag{S1}$$

Here r and z denote the radial and axial coordinates within the fiber, t stands for time, $\omega_{\text{pump1}}, k_{\text{pump1}}$ are the temporal frequency and axial wavenumber of the optical field, and $u_{\text{core}}(r)$ (in units of m-1) is the transverse profile of the core mode. The transverse profile is radially-symmetric, and normalized so that $2\pi\int_0^\infty \left|u_{\text{core}}(r)\right|^2 r\mathrm{d}r = 1$. Last, $A_{\text{pump1}}(z)$ (in V) represents the local complex magnitude of the first pump wave. A second, co-polarized and continuous optical pump field is counter-propagating in the core mode, in the negative $\hat{\mathbf{z}}$ direction:

$$E_{\text{pump2}}(r,z,t) = A_{\text{pump2}}(z)\exp\left(-\mathrm{j}k_{\text{pump2}}z - \mathrm{j}\omega_{\text{pump2}}t\right)u_{\text{core}}(r) + c.c \tag{S2}$$

In Supplementary Equation (S2), $A_{\text{pump2}}(z)$ represents the complex magnitude of the second pump wave, and k_{pump2} is its wavenumber. The optical frequency of the second pump wave is given by $\omega_{\text{pump2}} = \omega_{\text{pump1}} - \Omega$, where Ω is close to the Brillouin frequency shift Ω_{B} in the fiber. We denote the effective index of the core mode as n_{core}, so that $k_{\text{pump1,2}} = n_{\text{core}}\,\omega_{\text{pump1,2}}/c$ where c is the speed of light in vacuum. We assume that n_{core} is the same for all frequencies of interest.

Backward stimulated Brillouin scattering (SBS) interaction between the two pump fields generates a longitudinal acoustic wave of density fluctuations $\Delta\rho(r,z,t)$, which is co-propagating with E_{pump1} [S1]:

$$\Delta\rho(r,z,t) = B(z,\Omega)\exp\left(\mathrm{j}qz - \mathrm{j}\Omega t\right)u_{\text{ac}}(r) + c.c. \tag{S2}$$

Here $q = k_{\text{pump1}} + k_{\text{pump2}}$ is the acoustic wavenumber and $u_{\text{ac}}(r)$ is the transverse profile of a longitudinal acoustic mode that is guided by the core of the fiber, normalized to $2\pi\int_0^\infty \left|u_{\text{ac}}(r)\right|^2 r\mathrm{d}r = 1$. The transverse profile of the electrostrictive force induced by the two pump waves is radially-symmetric, hence the stimulated acoustic mode must maintain the same symmetry. The magnitude of the acoustic wave, in units of kg×m-2, is given by [S1]:

$$B(z,\Omega) = \varepsilon_0\gamma_e q^2 Q_{\text{core}}\frac{1}{\Omega_{\text{B}}^2 - \Omega^2 - \mathrm{j}\Omega\Gamma_{\text{B}}}A_{\text{pump1}}(z)A^*_{\text{pump2}}(z) \tag{S3}$$

In Supplementary Equation (S4) ε_0 is the vacuum permittivity, γ_e is the electrostrictive constant of silica, and $\Gamma_B \approx 2\pi\times30$ MHz represents the Brillouin linewidth in silica. Q_{core} [m-1] denotes the spatial overlap integral between the transverse profile of the optical intensity in the core mode and that of the acoustic mode:

$$Q_{\text{core}} \equiv 2\pi\int_0^\infty \left|u_{\text{core}}(r)\right|^2 u_{\text{ac}}^*(r)\, r\mathrm{d}r \qquad \text{(S4)}$$

Consider next a third continuous optical probe wave, which is co-propagating with E_{pump1} in the core optical mode of the fiber:

$$E_{\text{probe}}(r,z,t) = A_{\text{probe}}(z)\exp\left(\mathrm{j}k_{\text{probe}}z - \mathrm{j}\omega_{\text{probe}}t\right)u_{\text{core}}(r) + c.c \qquad \text{(S5)}$$

The complex magnitude of the probe wave is denoted by $A_{\text{probe}}(z)$, its optical frequency is $\omega_{\text{probe}} > \omega_{\text{pump1}}$, and its wavenumber k_{probe} equals $k_{\text{probe}} = n_{\text{core}}\,\omega_{\text{probe}}/c$. The combination of the probe optical field and the stimulated acoustic wave is associated with a nonlinear polarization term at optical frequency $\omega_{\text{probe}} - \Omega$, due to photo-elasticity [S1]:

$$\begin{aligned} P_{\text{NL}}(r,z,t) =& \varepsilon_0 \frac{\gamma_e}{\rho_0} B^*(z) A_{\text{probe}}(z) \times \\ &\times u_{\text{ac}}^*(r) u_{\text{core}}(r) \exp\left[\mathrm{j}\left(k_{\text{probe}} - q\right)z - \mathrm{j}\left(\omega_{\text{probe}} - \Omega\right)t\right] + c.c. \end{aligned} \qquad \text{(S6)}$$

Here ρ_0 is the density of silica. Note that $\left(k_{\text{probe}} - q\right) < 0$, hence the nonlinear polarization represents a wave perturbation propagating in the negative $\hat{\mathbf{z}}$ direction. The above nonlinear polarization can lead to scattering of the probe wave into a counter-propagating, fourth optical field of frequency $\omega_{\text{probe}} - \Omega$, provided that its wavenumber matches that of Supplementary Equation (S7). This requirement can be satisfied in the m^{th}-order cladding mode of the fiber, with effective index $n_{\text{clad}}^{(m)} < n_{\text{core}}$, if the following condition is met:

$$\begin{aligned} k_{\text{clad}}^{(m)} =& \frac{n_{\text{clad}}^{(m)}}{c}\left(\omega_{\text{probe}} - \Omega\right) = q - k_{\text{probe}} = \\ & \frac{n_{\text{core}}}{c}\left(\omega_{\text{pump1}} + \omega_{\text{pump1}} - \Omega - \omega_{\text{probe}}\right) \end{aligned} \qquad \text{(S8)}$$

Based on Supplementary Equation (S8), Brillouin dynamic grating (BDG) coupling to the cladding mode is optimal for the following optical frequency of the probe wave:

$$\omega_{\text{probe,opt}}^{(m)} = \frac{2n_{\text{core}}\omega_{\text{pump1}} - \left(n_{\text{core}} - n_{\text{clad}}^{(m)}\right)\Omega}{n_{\text{core}} + n_{\text{clad}}^{(m)}} \approx \frac{2n_{\text{core}}}{n_{\text{core}} + n_{\text{clad}}^{(m)}}\omega_{\text{pump1}} \qquad \text{(S7)}$$

which is also Equation (1) in the Main Text. Note that the second term in the numerator of Supplementary Equation (S9) is smaller than the first by seven orders of magnitude, hence the approximation made is a very good one. The frequency detuning between the co-propagating pump and probe waves at optimal coupling is given by:

$$\Delta\omega_{\text{opt}}^{(m)} \equiv \omega_{\text{probe,opt}}^{(m)} - \omega_{\text{pump1}} = \frac{n_{\text{core}} - n_{\text{clad}}^{(m)}}{n_{\text{core}} + n_{\text{clad}}^{(m)}}\omega_{\text{pump1}} \qquad \text{(S10)}$$

Supplementary Fig. 1 shows the calculated $n_{\text{clad}}^{(m)}$ for a 125 µm-diameter fiber in air [S2], and the optimal wavelength offset between the probe and a pump waves at 1550 nm, as functions of the cladding mode order *m*.

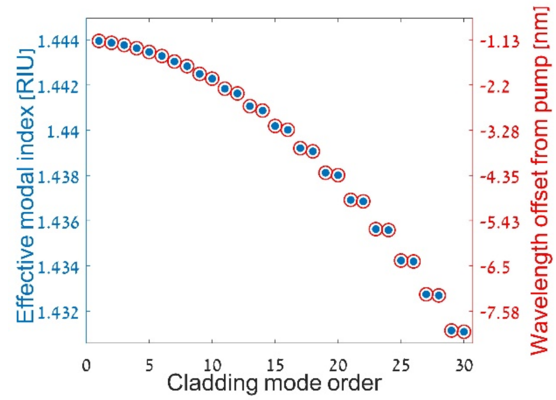

Supplementary Fig. 1. – Calculated effective index $n_{\text{clad}}^{(m)}$ (left axis), and wavelength offset between pumps and probe at maximum coupling of the probe wave to cladding modes (right axis, based on Supplementary Equation 10), as a function of cladding mode order *m*. A bare fiber with air outside the cladding is assumed. The cladding diameter is 125 µm.

The scattered field in the cladding mode may be expressed as:

$$\begin{aligned} & E_{\text{clad}}^{(m)}(r,z,t) = \\ & A_{\text{clad}}^{(m)}(z)\exp\left[-\mathrm{j}k_{\text{clad}}^{(m)}z - \mathrm{j}\left(\omega_{\text{probe}} - \Omega\right)t\right]u_{\text{clad}}^{(m)}(r) + c.c \end{aligned} \qquad \text{(S11)}$$

where $A_{\text{clad}}^{(m)}(z)$ is the complex magnitude of the scattered field and $u_{\text{clad}}^{(m)}(r)$ is the normalized transverse profile of the m^{th}-order cladding mode. The transverse profile of the cladding mode follows the radial symmetry of the optical core mode and the acoustic mode. The coupled nonlinear wave equations for the evolution of $A_{\text{probe}}(z)$ and $A_{\text{clad}}^{(m)}(z)$ take up the following form:

$$\begin{aligned} \frac{\mathrm{d}A_{\text{probe}}(z)}{\mathrm{d}z} =& \mathrm{j}\frac{\varepsilon_0\gamma_e^2 q^2\omega_{\text{probe}}Q_{\text{core}}Q_{\text{clad/core}}^{(m)}}{2nc\rho_0} \times \\ & \frac{A_{\text{pump1}}(z)A_{\text{pump2}}^*(z)}{\Omega_B^2 - \Omega^2 - \mathrm{j}\Omega\Gamma_B} A_{\text{clad}}^{(m)}(z)\exp\left(-\mathrm{j}\Delta k_{\text{BDG}}^{(m)}z\right) \end{aligned} \qquad \text{(S12)}$$

$$\begin{aligned} \frac{\mathrm{d}A_{\text{clad}}^{(m)}(z)}{\mathrm{d}z} =& -\mathrm{j}\frac{\varepsilon_0\gamma_e^2 q^2\omega_{\text{probe}}\left(Q_{\text{core}}Q_{\text{clad/core}}^{(m)}\right)^*}{2nc\rho_0} \times \\ & \frac{A_{\text{pump1}}^*(z)A_{\text{pump2}}(z)}{\Omega_B^2 - \Omega^2 + \mathrm{j}\Omega\Gamma_B} A_{\text{probe}}(z)\exp\left(\mathrm{j}\Delta k_{\text{BDG}}^{(m)}z\right) \end{aligned} \qquad \text{(S13)}$$

Here we use $n_{\text{clad}}^{(m)} \approx n_{\text{core}} \equiv n$ and $\left(\omega_{\text{probe}} - \Omega\right) \approx \omega_{\text{probe}}$. The term $Q_{\text{clad/core}}^{(m)}$ [m-1] stands for the spatial overlap integral between the transverse profiles of the core, cladding and acoustic modes:

$$Q_{\text{clad/core}}^{(m)} \equiv 2\pi\int_0^\infty u_{\text{ac}}(r)u_{\text{clad}}^{(m)}(r)u_{\text{core}}^*(r)\, r\mathrm{d}r \qquad \text{(S14)}$$

Lastly, the wavenumber mismatch term in Supplementary Equations (S12) and (S13) is defined as:

$$\Delta k_{\mathrm{BDG}}^{(m)} \equiv q - k_{\mathrm{probe}} - k_{\mathrm{clad}}^{(m)} = \frac{n_{core} + n_{\mathrm{clad}}^{(m)}}{c}\left(\omega_{\mathrm{probe}} - \omega_{\mathrm{probe,opt}}^{(m)}\right) \tag{S15}$$

For brevity, we rearrange the coefficients of Supplementary Equations (S12) and (S13):

$$\begin{aligned}&-\mathrm{j}\frac{\varepsilon_0\gamma_{\mathrm{e}}^2 q^2\omega_{\mathrm{probe}}Q_{\mathrm{core}}Q_{\mathrm{clad/core}}^{(m)}}{2nc\rho_0}\frac{1}{\Omega_{\mathrm{B}}^2-\Omega^2-\mathrm{j}\Omega\Gamma_{\mathrm{B}}} \approx \\ &-\mathrm{j}\frac{\varepsilon_0\gamma_{\mathrm{e}}^2 q^2\omega_{\mathrm{probe}}Q_{\mathrm{core}}Q_{\mathrm{clad/core}}^{(m)}}{2nc\rho_0}\frac{1}{-\mathrm{j}\Omega_{\mathrm{B}}\Gamma_{\mathrm{B}}}\frac{1}{1+\mathrm{j}2\Delta\Omega/\Gamma_{\mathrm{B}}} \\ &\frac{\varepsilon_0\gamma_{\mathrm{e}}^2 q^2\omega_{\mathrm{probe}}Q_{\mathrm{core}}Q_{\mathrm{clad/core}}^{(m)}}{2nc\rho_0\Omega_{\mathrm{B}}\Gamma_{\mathrm{B}}}\frac{1-\mathrm{j}2\Delta\Omega/\Gamma_{\mathrm{B}}}{1+\left(2\Delta\Omega/\Gamma_{\mathrm{B}}\right)^2} = \\ &C_{\mathrm{BDG,0}}Q_{\mathrm{core}}Q_{\mathrm{clad/core}}^{(m)}\frac{1-\mathrm{j}2\Delta\Omega/\Gamma_{\mathrm{B}}}{1+\left(2\Delta\Omega/\Gamma_{\mathrm{B}}\right)^2}\end{aligned} \tag{S16}$$

where $\Delta\Omega \equiv \Omega_{\mathrm{B}} - \Omega$, and:

$$C_{\mathrm{BDG,0}} \equiv \frac{\varepsilon_0\gamma_{\mathrm{e}}^2 q^2\omega_{\mathrm{probe}}}{2nc\rho_0\Omega_{\mathrm{B}}\Gamma_{\mathrm{B}}} \tag{S17}$$

We assume further that the two pump waves are undepleted in the short fiber under test. With the above definitions, we may rewrite Supplementary Equations (S12) and (S13):

$$\begin{aligned}\frac{\mathrm{d}A_{\mathrm{probe}}(z)}{\mathrm{d}z} = &-C_{\mathrm{BDG,0}}Q_{\mathrm{core}}Q_{\mathrm{clad/core}}^{(m)}A_{\mathrm{pump1}}A_{\mathrm{pump2}}^{*}\times \\ &\frac{1-\mathrm{j}2\Delta\Omega/\Gamma_{\mathrm{B}}}{1+\left(2\Delta\Omega/\Gamma_{\mathrm{B}}\right)^2}A_{\mathrm{clad}}^{(m)}(z)\exp\left(-\mathrm{j}\Delta k_{\mathrm{BDG}}^{(m)}z\right)\end{aligned} \tag{S18}$$

$$\begin{aligned}\frac{\mathrm{d}A_{\mathrm{clad}}^{(m)}(z)}{\mathrm{d}z} = &-C_{\mathrm{BDG,0}}\left(Q_{\mathrm{core}}Q_{\mathrm{clad/core}}^{(m)}\right)^{*}A_{\mathrm{pump1}}^{*}A_{\mathrm{pump2}}\times \\ &\frac{1+\mathrm{j}2\Delta\Omega/\Gamma_{\mathrm{B}}}{1+\left(2\Delta\Omega/\Gamma_{\mathrm{B}}\right)^2}A_{\mathrm{probe}}(z)\exp\left(\mathrm{j}\Delta k_{\mathrm{BDG}}^{(m)}z\right)\end{aligned} \tag{S19}$$

Due to the short lengths of fiber used, and the small spatial overlap between core and cladding modes $Q_{\mathrm{clad/core}}^{(m)}$, the coupling of power between E_{probe} and $E_{\mathrm{clad}}^{(m)}$ is very weak. Although $\left|A_{\mathrm{probe}}\right|^2 << \left|A_{\mathrm{pump1,2}}\right|^2$, we may still assume that changes in A_{probe} remain small (although nonzero). At that limit, the magnitude of the optical field that is coupled into the cladding mode by a BDG of length L_{BDG} is approximately given by:

$$\begin{aligned}A_{\mathrm{clad,out}}^{(m)} \approx\ & C_{\mathrm{BDG,0}}\left(Q_{\mathrm{core}}Q_{\mathrm{clad/core}}^{(m)}\right)^{*}A_{\mathrm{pump1}}^{*}A_{\mathrm{pump2}} \\ &\times\frac{1+\mathrm{j}2\,\Delta\Omega/\Gamma_{\mathrm{B}}}{1+\left(2\Delta\Omega/\Gamma_{\mathrm{B}}\right)^2}A_{\mathrm{probe}} \\ &\times\exp\left(\mathrm{j}\frac{\Delta k_{\mathrm{BDG}}^{(m)}L_{\mathrm{BDG}}}{2}\right)L_{\mathrm{BDG}} \\ &\times\mathrm{sinc}\left(\frac{\Delta k_{\mathrm{BDG}}^{(m)}L_{\mathrm{BDG}}}{2}\right)\end{aligned} \tag{S20}$$

The optical power coupled to the cladding mode is given by $P_{\mathrm{clad,out}}^{(m)} = 2nc\varepsilon_0\left|A_{\mathrm{clad,out}}^{(m)}\right|^2$ (see [S3]):

$$\begin{aligned}P_{\mathrm{clad,out}}^{(m)} &\approx \frac{2\varepsilon_0 nc C_{\mathrm{BDG,0}}^2\left|Q_{\mathrm{core}}\right|^2\left|Q_{\mathrm{clad/core}}^{(m)}\right|^2\left|A_{\mathrm{pump1}}\right|^2\left|A_{\mathrm{pump2}}\right|^2}{1+\left(2\Delta\Omega/\Gamma_{\mathrm{B}}\right)^2} \\ &\quad\times\left|A_{\mathrm{probe}}\right|^2 L_{\mathrm{BDG}}^2\mathrm{sinc}^2\left(\frac{\Delta k_{\mathrm{BDG}}^{(m)}L_{\mathrm{BDG}}}{2}\right) \\ &= \frac{C_{\mathrm{BDG,0}}^2\left|Q_{\mathrm{core}}\right|^2\left|Q_{\mathrm{clad/core}}^{(m)}\right|^2\left|A_{\mathrm{pump1}}\right|^2\left|A_{\mathrm{pump2}}\right|^2}{1+\left(2\Delta\Omega/\Gamma_{\mathrm{B}}\right)^2} \\ &\quad\times\mathrm{sinc}^2\left(\frac{\Delta k_{\mathrm{BDG}}^{(m)}L_{\mathrm{BDG}}}{2}\right)L_{\mathrm{BDG}}^2 P_{\mathrm{probe}} \\ &= \left(\frac{C_{\mathrm{BDG,0}}}{2nc\varepsilon_0}\right)^2\frac{\left|Q_{\mathrm{core}}\right|^2\left|Q_{\mathrm{clad/core}}^{(m)}\right|^2 P_{\mathrm{pump1}}P_{\mathrm{pump2}}}{1+\left(2\Delta\Omega/\Gamma_{\mathrm{B}}\right)^2} \\ &\quad\times\mathrm{sinc}^2\left(\frac{\Delta k_{\mathrm{BDG}}^{(m)}L_{\mathrm{BDG}}}{2}\right)L_{\mathrm{BDG}}^2 P_{\mathrm{probe}}\end{aligned} \tag{S21}$$

Here $P_{\mathrm{probe}} = 2nc\varepsilon_0\left|A_{\mathrm{probe}}\right|^2$ is the input power of the probe wave, and $P_{\mathrm{pump1,2}} = 2nc\varepsilon_0\left|A_{\mathrm{pump1,2}}\right|^2$ are the input powers of the two pump waves. The reflected power obtains a maximum value when the frequency offset Ω between the two pump waves matches exactly the Brillouin frequency shift Ω_{B} ($\Delta\Omega = 0$), and the frequency of the probe equals $\omega_{\mathrm{probe,opt}}^{(m)}$ ($\Delta k_{\mathrm{BDG}}^{(m)} = 0$). The reflectivity bandwidth with respect to Ω equals the Brillouin linewidth Γ_{B}. The bandwidth with respect of ω_{probe} is inversely proportional to the BDG length L_{BDG}. The maximum BDG reflectivity into the cladding mode may be expressed as:

$$\begin{aligned}R_{\max}^{(m)} &\equiv \left.\frac{P_{\mathrm{clad,out}}^{(m)}}{P_{\mathrm{probe}}}\right|_{\Delta\Omega=\Delta k_{\mathrm{BDG}}^{(m)}=0} \approx \\ &\left(\frac{C_{\mathrm{BDG,0}}}{2nc\varepsilon_0}\right)^2\left|Q_{\mathrm{core}}\right|^2\left|Q_{\mathrm{clad/core}}^{(m)}\right|^2 P_{\mathrm{pump1}}P_{\mathrm{pump2}}L_{\mathrm{BDG}}^2 \\ &= D_{\mathrm{BDG,0}}^2\left|Q_{\mathrm{core}}\right|^2\left|Q_{\mathrm{clad/core}}^{(m)}\right|^2 P_{\mathrm{pump1}}P_{\mathrm{pump2}}L_{\mathrm{BDG}}^2,\end{aligned} \tag{S22}$$

where the coefficient $D_{\mathrm{BDG,0}}$ (in units of m×W^{-1}) is defined as:

$$D_{\mathrm{BDG,0}} \equiv \frac{\gamma_{\mathrm{e}}^2 q^2\omega_{\mathrm{probe}}}{4n^2c^2\rho_0\Omega_{\mathrm{B}}\Gamma_{\mathrm{B}}} \approx \frac{\gamma_{\mathrm{e}}^2}{2c^3 nv\rho_0\Gamma_{\mathrm{B}}}\omega^2 \tag{S23}$$

Here we used $q = \Omega / v$ with v the velocity of longitudinal acoustic waves, and we approximated $\Omega \approx \Omega_B \approx 2n\omega_{\text{pump1}} v/c$ and $\omega_{\text{pump1}} \approx \omega_{\text{probe}}$ denoted by ω.

The power reflectivity to the cladding mode is weaker than that of a BDG in a polarization maintaining fiber by a transverse efficiency factor $\eta^{(m)} \equiv \left|Q^{(m)}_{\text{clad/core}}\right|^2 / \left|Q_{\text{core}}\right|^2$. Supplementary Fig. 2 shows the numerically calculated $\eta^{(m)}$ as a function of cladding mode order m. The cladding radius was taken as 125 μm, the core radius was 4.1 μm, and the mode-field diameter of the core mode $\left|u_{\text{core}}(r)\right|^2$ was 9.7 μm. Calculations were repeated twice: first under the assumption that the transverse profile of the acoustic mode $u_{\text{ac}}(r)$ is proportional to that of optical intensity in the core mode $\left|u_{\text{core}}(r)\right|^2$, and again for uniform $u_{\text{ac}}(r)$ within the core. The former model follows the transverse profile of the electrostrictive driving force, whereas the latter matches that of permanent fiber Bragg gratings [S2],. Differences between the two sets of results are small.

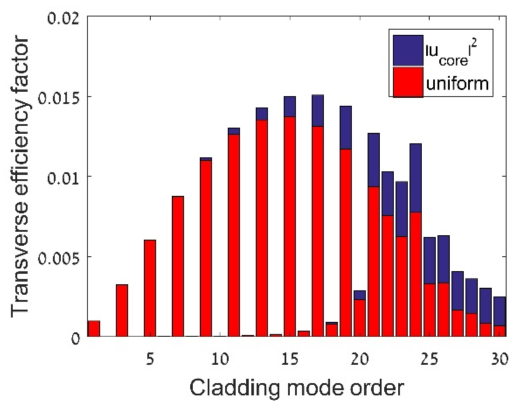

Supplementary Fig. 2. – Calculated transverse efficiency factor of Brillouin dynamic grating coupling as a function of cladding mode order. Blue: the transverse profile of the acoustic mode was assumed to be proportional to the optical intensity profile of the optical core mode: $u_{\text{ac}}(r) \propto \left|u_{\text{core}}(r)\right|^2$. Red: the transverse profile of the acoustic mode $u_{\text{ac}}(r)$ was assumed to be uniform across the core.

The analysis suggests that BDG coupling is the most efficient for odd cladding mode orders between 13 and 19 [S2]. Note that the even cladding modes are characterized by zero optical field on the fiber axis. The radial profiles of the cladding mode fields oscillate with periods that become shorter as the modal order increases. For low-order even modes, the field remains very weak throughout the extent of the core and the transverse efficiency of Brillouin dynamic grating coupling vanishes accordingly. For higher-order even modes, radial variations in the field profile are gradually pushed into the core, giving rise to somewhat larger transverse overlap with the dynamic gratings.

The highest transverse efficiency is expected for mode m = 17. However, even $\eta^{(17)}$ is only about 1.5%. The reflectivity $R^{(17)}_{\max}$ of few-cm long BDGs into the cladding is weak: on the order of 100 ppm for few Watts of pumps power. Nevertheless, coupling spectra are successfully used in distributed sensing outside the cladding (see Main Text). Due to the difficulty of collecting light from the cladding modes, we monitor the process instead by measuring the changes in the transmitted probe power: $\Delta P_{\text{probe}} = -P^{(m)}_{\text{clad,out}}$.

2. Localization of steady state stimulated Brillouin scattering interactions through phase coding of pump waves

The localization of stimulated Brillouin scattering interactions through the phase coding of two optical waves has been described in detail in several works [S4][S5]. The principle is briefly repeated here for completeness. The reader is referred to a recent review [S6]. In this technique, the two pump fields are no longer continuous. The complex magnitude of pump field E_{pump1} is modulated at its point of entry into the fiber ($z = 0$), so that:

$$A_{\text{pump1}}(z,t) = A^{(0)}_{\text{pump1}} f\left(t - \frac{z}{v_g}\right) \tag{S24}$$

In Supplementary Equation (S24), $A^{(0)}_{\text{pump1}}$ is a constant magnitude, v_g is the group velocity of light in the fiber, and $f(t)$ is a modulation function of the optical source with unity norm: $\left|f(t)\right|^2 = 1$. The counter-propagating E_{pump2} is modulated by the same function $f(t)$ at its launch point in the opposite end of the fiber $z = L$, so that:

$$A_{\text{pump2}}(z,t) = A^{(0)}_{\text{pump2}} f\left(t - \frac{L-z}{v_g}\right) \tag{S25}$$

Here $A^{(0)}_{\text{pump2}}$ represents a second constant magnitude. Due to the modulation of the pump waves, the magnitude of the stimulated acoustic density perturbation generally does not reach a steady state. The instantaneous acoustic magnitude is given by [S6]:

$$\begin{aligned} B(z,t) = {} & \mathrm{j}\varepsilon_0 \gamma_e q^2 Q_{\text{core}} A^{(0)}_{\text{pump1}} \left(A^{(0)}_{\text{pump2}}\right)^* \times \\ & \int_{-\infty}^{t} \exp\left[\Gamma_{\text{ac}}(\Omega)\cdot(t-t')\right] \times \\ & f\left(t' - \frac{z}{v_g}\right) f\left[t' - \frac{z}{v_g} + \theta(z)\right] \mathrm{d}t' \end{aligned} \tag{S26}$$

In Supplementary Equation (S26) we defined a complex linewidth $\Gamma_{\text{ac}}(\Omega) \equiv \mathrm{j}\left(\Omega_B^2 - \Omega^2 - \mathrm{j}\Omega\Gamma_B\right) / 2\Omega s$ and a position-dependent time lag $\theta(z) \equiv (2z - L)/v_g$. The complex linewidth reduces to $\frac{1}{2}\Gamma_B$ when $\Omega = \Omega_B$.

Let us denote the auto-correlation function of the modulation waveform $f(t)$ as $C_f(\xi)$, where ξ is a delay variable. Supplementary Equation (S26) suggests that the expectation value of the stimulated acoustic wave at z is closely related with $C_f\left[\theta(z)\right]$. Note, however, that the acoustic wave magnitude does not perfectly follow the auto-correlation function, due to the exponential weighing window $\exp\left[\Gamma_{\text{ac}}(\Omega)\cdot(t-t')\right]$ that is associated with electrostrictive stimulation.

Following on earlier works [S4-S6], the modulation function $f(t)$ is chosen as a repeating binary phase sequence, with symbol duration T and a period of N bits:

$$f(t) = \sum_n a_n \mathrm{rect}\left(\frac{t-nT}{T}\right) \qquad \text{(S27)}$$

Here $\mathrm{rect}(\xi)=1$ if $|\xi| \le 0.5$ and equals zero elsewhere, and a_n is the value of bit n in the sequence. The bit duration T is taken to be much shorter than the Brillouin lifetime: $T \ll 1/\Gamma_\mathrm{B}$. The values of a_n are those a prefect Golomb code: a class of binary phase sequences that are designed for zero side-lobes of their cyclic auto-correlation functions [S6][S7]. Due to the phase modulation, a correlation peak forms at the center of the fiber $z = L/2$ ($\theta = 0$), where the magnitude of the acoustic wave reaches its steady-state value of Supplementary Equation (S4). The width of the resulting BDG L_BDG equals $\frac{1}{2} v_g T$. Periodic, higher-order peaks appear at positions $z = L/2 + M \cdot N \cdot L_\mathrm{BDG}$, where M is a positive or negative integer.

Outside the correlation peaks, the magnitudes of the stimulated acoustic waves are rapidly fluctuating, as the arguments within the integral of Supplementary Equation (S26) may assume positive or negative values. The expectation values of the acoustic wave magnitudes outside the peak equal zero for all times. Therefore, in principle, measurements of E_probe at the end of the fiber may retrieve the local BDG spectrum at the position of the correlation peak only. However, even though off-peak Brillouin interactions are zero on average, their instantaneous magnitudes are non-zero with a finite variance [S6]. Off-peak Brillouin interactions contribute noise to the measurements of BDG coupling spectra [S6].

Measurements of BDGs with phase-coded pump waves are unambiguous for fiber lengths L that are shorter than $N \cdot L_\mathrm{BDG}$. Since the repeating phase-modulation sequence can be chosen at any length, the range of unambiguous measurements may be arbitrarily long, with no effect on spatial resolution. In many realizations of the concept, the fiber paths leading the two pump waves into the measurement section of interest are deliberately imbalanced, so that a high-order correlation peak ($M \gg 1$) is in overlap with the region of interest [S8]. With this choice, the position of the correlation peak can be conveniently scanned through small-scale variations in the bit duration T [S8].

A distributed map of BDG coupling spectra as a function of position can be obtained by scanning the location of the correlation peak position, one resolution point at a time, and then scanning the optical frequency of the probe wave ω_probe at each position. The technique has been widely employed in distributed Brillouin optical correlation domain analysis (B-OCDA) sensing of temperature and axial strain [S5][S6]. It was also used in BDGs over polarization maintaining fibers, towards sensing, all-optical variable delay lines and microwave-photonic filters [S4][S9-S11]. In this work, phase coding of the two pump waves is used to obtain distributed mapping of local coupling spectra between the optical probe field and cladding modes of the fiber under test (see Main Text).

References

1. R. W. Boyd, Nonlinear Optics 3rd Edition, (Academic, 2008).
2. T. Erdogan, "Cladding-mode resonances in short- and long period fiber grating filters," J. Opt. Soc. Am. A **14**, 1760-1773 (1997).
3. A. Bergman, L. Yaron, T. Langer, and M. Tur, "Dynamic and distributed slope-assisted fiber strain sensing based on optical time-domain analysis of Brillouin dynamic gratings," J. Lightwave Technol. **33**, 2611–2616 (2015).
4. Y. Antman, N. Primerov, J. Sancho, L. Thevenaz, and A. Zadok, "Localized and stationary dynamic gratings via stimulated Brillouin scattering with phase modulated pumps," Opt. Express **20**, 7807-7821 (2012).
5. A. Zadok *et al*., "Random-access distributed fiber sensing," Laser Photon. Rev. **6**, L1-L5 (2012).
6. A. Zadok, E. Preter, and Y. London, "Phase-Coded and Noise-Based Brillouin Optical Correlation-Domain Analysis," Appl. Sci. **8**, 1482 (2018).
7. S.W. Golomb, "Two-valued sequences with perfect periodic autocorrelation," IEEE Trans. Aerosp. Electron. Syst. **28**, 383–386 (1992).
8. A. Ben-Amram, Y. Stern, Y. London, Y. Antman, and A. Zadok, "Stable closed-loop fiber-optic delay of arbitrary radio-frequency waveforms," Opt. Express **23**, 28244-28257 (2015).
9. J. Sancho *et al*., "Tunable and reconfigurable multi-tap microwave photonic filter based on dynamic Brillouin gratings in fibers," Opt. Express **20**, 6157–6162 (2012).
10. Y. Antman *et al.*, "Experimental demonstration of localized Brillouin gratings with low off-peak reflectivity established by perfect Golomb codes," Opt. Lett. **38**, 4701–4704 (2013).
11. A. Bergman, and M. Tur, "Brillouin dynamic gratings - a practical form of Brillouin enhanced four wave mixing in waveguides: the first decade and beyond," Sensors **18**, 2863 (2018).